Review of Scientific Instruments

A compact setup for broadband polarization tomography

Yujia Yuan,[1,2] Sai S. Venuturumilli,[1,3] Michael Li,[1,2] Sema Kuru,[1,3] Paul Anderson,[1,3] Behrooz Semnani,[1,3] and Michal Bajcsy[1,2,3]
[1)] *Institute for Quantum Computing, University of Waterloo, Waterloo, ON, N2L3G1, Canada*
[2)] *Department of Engineering, University of Waterloo, Waterloo, ON, N2L3G1, Canada*
[3)] *Department of Science, University of Waterloo, Waterloo, ON, N2L3G1, Canada*

(*Electronic mail: y246yuan@uwaterloo.ca)

(Dated: 14 September 2021)

Abstract: Polarizatoin Tomography(PT) is used to reconstruct the quantum state. In this paper we first introduce the convention taken in our laboratory that is consistent with the electric field theory and Poincare Sphere(PS). Followed by is our compact design of the apparatus that takes only 20cm^2 area on the optics table that can do broadband tomography. Finally we demonstrate that the setup gives results with high purity and fidelity.

INTRODUCTION

PT is used to reconstruct the polarization state by the information of how much content is in each component[1]. Conventional PT setups[2] contain three beam splitters extracting specific polarizations and six power meters to measure how much power is in each polarization. The advantage of this setup is that it can continuously measuring polarization states at a fast speed because there is no mechanical part.

However, such a design is expensive and bulky because copies of the same devices are used. In this paper we discuss our implementation of a compact PT setup. With piezoelectric motors that rotate accurately, we only need one Half Waveplate(HWP), one Quarter Waveplate(QWP), one linear polarizer(LP) and one power meter.

The first sections are to strictly define conventions we use in our lab. There are a slew of literature describing polarization tomography, so does the Poincare Sphere. However, most of them fail to establish a simple visualization how the waveplates evolve states on the sphere, with clearly defined conventions. Some seemingly trivial confusions frequently leads to errors. In this paper, we will give a concise overview of all the strictly defined conventions used in our lab.

To visualize polarization states, we introduce the Poincare Sphere(PS) that represents polarization states in a simple way. PS is also a straightforward way of understanding the transformations let by waveplates, much more simple than matrix methods[3].

Further more, we show that the system can use a spectrometer instead of a power meter as the detector, thus achieving broadband tomography with a compact setup that is otherwise bulky and expensive.

TOMOGRAPHY CONVENTIONS

All waves propagating to +z direction can be decomposed into superposition of plane waves with the form

$$\vec{E} = (E_x\hat{x} + E_y\hat{y})e^{i(kz-\omega t)} \tag{1}$$

We can also represent it in Jone's vector: (E_x, E_y). Waveplates are optical components that introduce a phase retardance to the light passes through its slow axis, compared to that passes through its fast axis. If we decompose any incident light with pure polarization that passes through a waveplate, the resulting wave is

$$\vec{E} = (E_f\hat{f} + e^{i\phi}E_s\hat{s})e^{i(kz-\omega t)} \tag{2}$$

and its the matrix formalism of the phasor is:

$$\hat{E} = \begin{pmatrix} 1 & 0 \\ 0 & e^{i\phi} \end{pmatrix} \quad \phi \in \mathbf{R}^+ \tag{3}$$

Where $\phi = \pi/2$ for half waveplate and $\phi = \pi/4$ for quater waveplate. When the fast axis is aligned to x-axis, the waveplates are in the "zero" position. The angle of rotation is defined as the angle rotated counterclockwise if we look at the waveplate from the source of light to the direction of propagation.

We set horizontally polarized wave to be (1,0) state. Diagonal state $|D\rangle$ is when we look along the propagartion direction of the incident light, the superposition oscillates 45^o counterclockwise to the horizontal axis. For circularly polarization, we also look from the direction of propagation. Then the direction of rotation is represented by the Hand-rules. We summarize the ket representations and their matrix notations in Table I.

Ket	$\|H\rangle$	$\|V\rangle$	$\|D\rangle$	$\|A\rangle$	$\|L\rangle$	$\|R\rangle$
Matrix	$\begin{pmatrix}1\\0\end{pmatrix}$	$\begin{pmatrix}0\\1\end{pmatrix}$	$\frac{1}{\sqrt{2}}\begin{pmatrix}1\\1\end{pmatrix}$	$\frac{1}{\sqrt{2}}\begin{pmatrix}1\\-1\end{pmatrix}$	$\frac{1}{\sqrt{2}}\begin{pmatrix}1\\i\end{pmatrix}$	$\frac{1}{\sqrt{2}}\begin{pmatrix}1\\-i\end{pmatrix}$

TABLE I. Corresponding ket and matrix notations

It is also common to write the states in terms of density matrices ρ, especially when mixed states are a consideration.

I. POINCARE SPHERE

In this project, we do encounter mixed states. Thus density matrix is used instead of kets. Another advantage of using density matrix is that we can construct the Bloch Sphere[4] accordingly for a better visualization of state transformations.

Fig. 1 is the Poincare Sphere. The Poincare Sphere is equivalent to the Bloch Sphere, with slightly different notations for

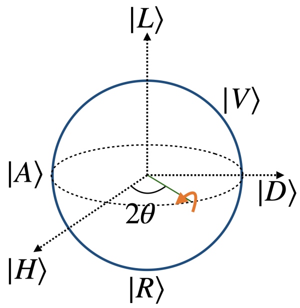

FIG. 1. Poincare Sphere for polarization states. Labels besides the axis are the pure states represented by corresponding axes. θ is the angle waveplates that can be used to "rotate" the sphere.

x and z axis to accommodate the convention that the x axis represents polarization state $|H\rangle$, the "baseline" we use in this project.

Pure states in Table I can be represented by directions along axis shown in Fig.1. For superposed or mixed states, Pauli Bases and S Parameters are crucial to defining positions on the sphere. Pauli Bases for the sphere are defined below. Again the order of σ_1 and σ_3 are switched, compared to the bases used by the Bloch Sphere.

$$\sigma_0 = \begin{pmatrix} 1 & 0 \\ 0 & 1 \end{pmatrix} \quad \sigma_1 = \begin{pmatrix} 1 & 0 \\ 0 & -1 \end{pmatrix} \quad \sigma_2 = \begin{pmatrix} 0 & -i \\ i & 0 \end{pmatrix} \quad \sigma_3 = \begin{pmatrix} 0 & 1 \\ 1 & 0 \end{pmatrix} \tag{4}$$

Any single-qubit density matrix ρ can be uniquely represented by the linear combination of σ bases:

$$\rho = \frac{1}{2S_0} \sum_{i=0}^{3} S_i \sigma_i \tag{5}$$

Where S_i are the overlap between the density matrix and Pauli Matrices that can be calculated by

$$S_i \equiv \mathrm{Tr}\{\sigma_i \rho\} \tag{6}$$

For all pure states,

$$\sum_{i=1}^{3} S_i^2 = S_0 \tag{7}$$

while for mixed states,

$$\sum_{i=1}^{3} S_i^2 < S_0 \tag{8}$$

It is also a common practice to normalize each S parameter by dividing S_0, so $S_0 = 1$ and parameters are power-independent. We adopt the normalized parameters in this paper since now on. Then normalized $S1, S2$ and $S3$ are x, y, z(or H, D, L) coordinates of the sphere. Thus each pure state that can be described by a ket $|\psi\rangle$ has a bijection on the surface of the sphere, each mixed state that cannot be expressed in a ket has a bijection inside the cavity of the sphere. If the state is completely mixed, it is at the center of the sphere.

Physically, each of the S parameters can be measured by specific pairs of projective measurements[1]:

$$\begin{aligned} P_0 &= P_{|H\rangle} + P_{|V\rangle} \\ P_1 &= P_{|H\rangle} - P_{|V\rangle} \\ P_2 &= P_{|D\rangle} - P_{|A\rangle} \\ P_3 &= P_{|L\rangle} - P_{|R\rangle} \end{aligned} \tag{9}$$

where $P_{|\psi\rangle}$ is the power of polarization state $|\psi\rangle$. In which P_0 is also the total power of the source, if the transmission efficiency and retardance of optical elements are assumed to be ideal. The four power parameters are just the un-normalized S parameters. Hence we have:

$$S_i = P_i / P_0 \tag{10}$$

If there are waveplates on the route of light transmission, the Poincare Sphere rotates along the line 2θ from $|H\rangle$ on the $|H\rangle|D\rangle$ plane by their retardances, as shown by Figure 1. For example, if a quarter waveplate has its fast axis 45 degrees from horizontal, it rotates the sphere by $\pi/2$, around $|D\rangle$ according to the Right-hand Rule. Thus $|L\rangle$ before the quarter waveplate becomes $|H\rangle$ after it. It is proven[5] that a half waveplate(HWP) together with a quarter waveplate(QWP) can rotate any point on the surface of the Poincare Sphere to $|H\rangle$ by different θs.

POLARIZATION TOMOGRAPHY SETUP

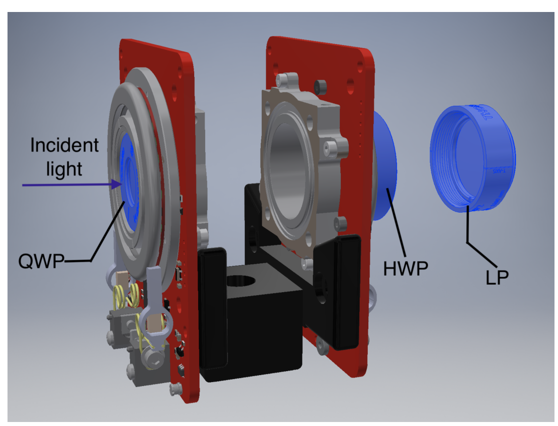

FIG. 2. 3D assembly of out tomography setup. The black support is designed by ourselves that holds two motors in a compact fashion. All other components are from Thorlabs. Motors are installed back to each other. The QWP is AQWP05M-980, the HWP is AHWP10M-980 and the LP is LPNIR050.

One conventional setup for measuring powers of each polarization state is to adopt multiple light paths and deploy one powermeter on each route. The major disadvantages are the bulky setup and sometimes expensiveness of the powermeter.

Our compact tomography setup that only requires one powermeter is shown in Fig. 2. The footprint of the two motors is less than 10cm^2. Polarizer and waveplates are all achromatic, with their working range 690-1200nm. Extinction ratio of the polarizer is > 1000. This allows the setup compatible with a broad wavelength range. Piezo motors we select have a built-in encoder that allows us to do feedback and reach a high precision: the error with feedback can be $< 0.5^o$.

According to the convention set in the previous section, horizontal axis is the baseline of the setup. So polarizer is aligned to pass $|H\rangle$, and fast axes of waveplates are aligned horizontally initially.

If the two waveplates rotate by specific amounts, corresponding polarization states can be transformed to $|H\rangle$ according to the rule stated in the previous section. By passing through the horizontally aligned polarizer, only $|H\rangle$ component is left and thus we can measure the power of any state. Table II lists all the angles of the two waveplates for coordinate states to be transformed to $|H\rangle$. The values in the table are not the only ones apply. For example, when the HWP is aligned to 22.5^o, it has the same effect as when it is aligned to 67.5^o. Notice that two motors are installed back to each other for compactness. So the direction of rotation should be opposite for the HWP.

Power of	QWP	HWP
$\|H\rangle$	0	0
$\|V\rangle$	0	45^o
$\|D\rangle$	45^o	22.5^o
$\|A\rangle$	45^o	67.5^o
$\|L\rangle$	45^o	0
$\|R\rangle$	45^o	45^o

TABLE II. Angles of waveplates to transform different states to $|H\rangle$.

If the powermeter is placed after the LP, it can measure the power in all the states and reconstruct the point on the Poincare Sphere through equation 5 and 6.

EXPERIMENTAL RESULTS

$$p = \sqrt{S_1^2 + S_2^2 + S_3^2} \tag{11}$$

It is a measure how mixed the input light is. As described before, when the state is pure, $p = 1$ and when the state is completely mixed, $p = 0$. If a light is polarized, we should expect to have $p \approx 1$. Interestingly, sometimes we get the purity slightly above 1, which is not physical. The reason for this is that the power fluctuates, and may make $|H\rangle$ and $|V\rangle$ slightly lower during the measurement. Because the normalization factor $S_0 = P_H + P_V$, other terms are scaled up a little. If we see a > 1 purity, we just normalize every S parameters again with purity and assume the state is pure.

In addition to the purity, we have fidelity a measurement about how much the reconstructed state overlaps with the actual state[6]:

$$F = \frac{1}{2}\left(\vec{S}_{prep} \cdot \vec{S}_{recon}\right) \tag{12}$$

Both of the S vectors are normalized with p so that each of them has the length of 1. Doing so allows us to separate the effect of purity from consideration of fidelity.

"Correctness" of measurements is the product of purity and fidelity. With the setup described in the previous section, measurements can be carried out. Motors communicate with the controlling computer through serial port by their communication protocols that can be found in[7]. Powermeter used is PM16-130 from Thorlab. It can communicate with computers through Python. Thus automation can be implemented. Purity is constantly 1. When the input is $|H\rangle$, S_1 measured is 0.997; when the input is $|V\rangle$, $S_1 = 0.991$; when the input is $|D\rangle$, $S_2 = 97.4$. So the simple tests show that the "correctness" of results are greater than 95%, which is pretty accurate.

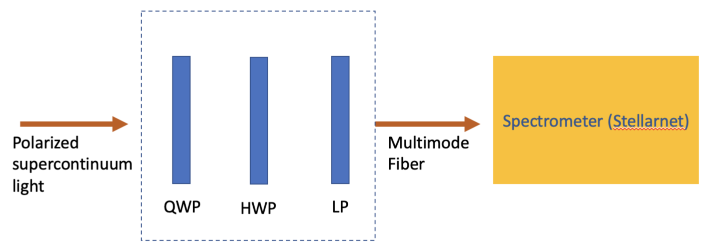

FIG. 3. Setup of the broadband tomography. Light source is selected to be a supercontinuum laser containing frequency from 200nm to 900nm. We only focus on 800-900nm. Light passing the LP is collected by a multimode fiber and sent to the spectrometer BLK-CXR-SR for analyzing. The fiber M91L01 has core diameter 200um[8] and its supported wavelength range is 250-1200nm.

All the optical components are achromatic. Thus in addition to the powermeter, we can use a spectrometer as the detector and perform polarization tomography for multiple wavelengths respectively at the same time. The setup is shown in Fig. 3.

The spectrometer uses the drive provided by StellarNet and can send data through MATLAB. Thus automation with the spectrometer can also be implemented. The only issue is that the drive only support Python 2 environment and its USB port connectivity is finicky at times.

Fig.4 is the broadband tomography result of a horizontally polarized incident light. The purity is constantly 0.96. Our assumption why it does not go to 1 is because of the ambient radiation. 850nm is in the infra-red region, ambient radiation in the form of heat might add some noise to the light composition and it becomes more mixed.

S_1 is close to the purity, which means most of the power goes into $|H\rangle$. S_2 and S_3 are not strictly zero. This may due to the slight misalignment when we were doing the measurement. Non-ideality of waveplates is another probable cause. The retardance of the HWP, for example, is 0.26λ instead of 0.25λ. Thus the transformation of states is not perfect.

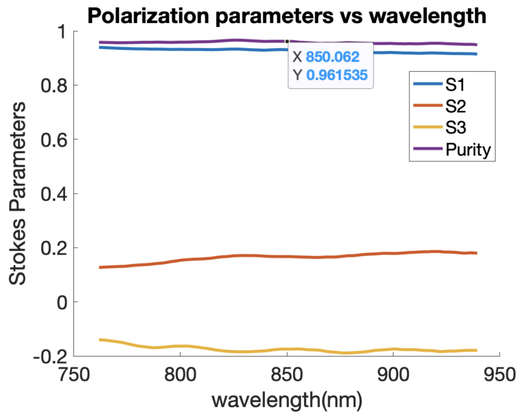

FIG. 4. S parameters and purity versus wavelength plot. Input is a horizontally polarized supercontinuum laser beam with spectrum 500-900nm. The beam is then tested with our setup. The integration time of the spectrometer is 0.5 seconds.

To see the fidelity, we plot the Poincare Sphere. Our software allows us to choose any wavelength in Fig. 4 and plot the Poincare Sphere accordingly. Here we choose 850nm for demonstration. Fig. 5 is the Poincare Sphere, with a red line indicating the vector of the point. From the plot we see that the point is very close to $|H\rangle$. The fidelity is ≈ 0.96, which proves the visualization.

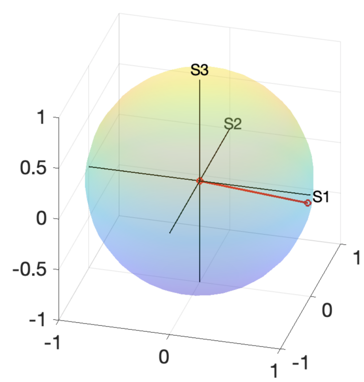

FIG. 5. Poincare Sphere representation for 850nm light with the setup same as that of Figure 4. S1, S2 and S3 are normalized with respect to S0 for a relative value. Length of the red line is the purity. Position of the red hollow dot is the polarization state

To show that the waveplates rotates the Poincare Sphere in the right way, we add a HWP before our setup to turn $|H\rangle$ into $|A\rangle$ and do the measurement.

Fig. 6 shows that the resulting state is close to $S_2 = -1$, which validates both our theory and the tomography system.

To quantify the fidelity of all linear states, we prepare linear polarizations by controlling horizontally polarized light with another HWP AHWP10M-980. The HWP transforms $|H\rangle$ into other states according to the Right-hand rotation rule. Results are listed in Table III.

Therefore, we make an conclusion that the compact setup with two motors can perform polarization tomography reasonably well with a high purity and fidelity. We can also extend the design so that broadband tomography is achievable.

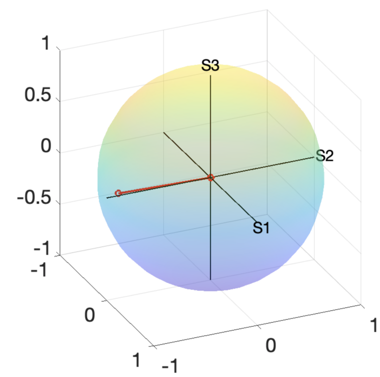

FIG. 6. Poincare Sphere for 850nm light with a HWP having its fast axis 67.5^o to the horizontal axis before the device and after the polarized source.

State	H	V	D	A
Fidelity	96.8%	96.2%	99.7%	99.8%

TABLE III. Fidelity of linear polarization states. Polarization are controlled by a broadband HWP AHWP10M-980.

CONCLUSION

In the first two sections we strictly define the conventions used in our lab, eliminating confusions in the directions or definitions. And we introduce the concept of Poincare Sphere, how polarization states can be represented by points on the sphere and how the points move under the unitary transformation incurred by waveplates.

We implement the tomography device according to the conventions created, and demonstrate that the reconstructed state is accurate, with both the fidelity and purity higher than 95%. The setup is small, saving both the optical table space and cost of multiple powermeters. In addition, we show that the system can be re-configured so broadband tomography is feasible.

There are some future works that may improve the existing design. First of all, the waveplates are not ideal. For example, slow-axis retardance is close to 0.26λ for the QWP instead of the ideal 0.25λ. As a result, the states but $|H\rangle$ we measure are not exactly accurate ones. There is a bit deviation from the theoretical states. In addition, the spectrometer has a limited resolution. Even with an input pulse whose linewidth is $\approx 50kHz$, it displays a Gaussian with 6nm FWHM. As a result, it is difficult to use the spectrometer for broadband polarization tomography that require fine linewidth to resolve thin spectral lines. We may switch to a spectrometer with a higher resolution or try to see whether we can implement the de-convolution to extract delta pulses from Gaussians.

ACKNOWLEDGMENTS

This research was undertaken in part due to funding from the Canada First Research Excellence Fund. In addition, this work was supported by Industry Canada, an NSERC Discovery grant, and Ontario's Ministry of Innovation Early Researcher Award. The authors also thank the Institute for Quantum Computing for support with the 3D printers.

DATA AVAILABILITY STATEMENT

Relevant data of this project can be found in the GitHub link https://github.com/YJ-Yuan/Broadband-Tomography. Further details can be obtained from the corresponding author on demand.

REFERENCES

[1] J. B. Altepeter, D. F. James, and P. G. Kwiat, "4 qubit quantum state tomography," Quantum State Estimation , 113–145 (2004).

[2] O. Bayraktar, M. Świłło, C. Canalias, and G. Bjork, "Quantum-polarization state tomography," Physical Review A **94**, 020105 (2016).

[3] E. Collett, (SPIE PRESS BOOK, 2005).

[4] D. A. Steck, "Quantum and atom optics," (2007), chapter 5.4 Bloch Sphere.

[5] M. V. Preite, V. Sorianello, G. De Angelis, M. Romagnoli, and P. Velha, "Geometrical representation of a polarisation management component on a soi platform," Micromachines **10**, 364 (2019).

[6] S. K. Pang, "Efficient polarisation measurement for quantum cryptography," National University of Singapore (2005).

[7] Thorlabs, "Communications protocol," Available at "`https://www.thorlabs.com/software\_pages/ViewSoftwarePage.cfm?Code=ELL`" ().

[8] Thorlabs, "Multimode hybrid fiber optic patch cables," Available at "`https://www.thorlabs.com/newgrouppage9.cfm?objectgroup\_id=5016\&pn=M91L01#7552`" ().

[9] P. Kaye, R. Laflamme, and M. Mosca, *An introduction to quantum computing* (Oxford University Press, 2007).